
Adversarial Moment-Matching Distillation of Large Language Models

Chen Jia

SI-TECH Information Technology
jiachenwestlake@gmail.com

Abstract

Knowledge distillation (KD) has been shown to be highly effective in guiding a student model with a larger teacher model and achieving practical benefits in improving the computational and memory efficiency for large language models (LLMs). State-of-the-art KD methods for LLMs mostly rely on minimizing explicit distribution distance between teacher and student probability predictions. Instead of optimizing these mandatory behaviour cloning objectives, we explore an imitation learning strategy for KD of LLMs. In particular, we minimize the imitation gap by matching the action-value moments of the teacher’s behavior from both on- and off-policy perspectives. To achieve this action-value moment-matching goal, we propose an adversarial training algorithm to jointly estimate the moment-matching distance and optimize the student policy to minimize it. Results from both task-agnostic instruction-following experiments and task-specific experiments demonstrate the effectiveness of our method and achieve new state-of-the-art performance.

1 Introduction

Large language models (LLMs) like GPT-4 [1] and LLaMA [32] have revolutionized natural language processing, significantly enhancing the quality of text generation across various tasks. This success is largely due to the extensive scale of training data and the substantial increase in model parameters [17]. However, the high computational and memory requirements of these models present significant challenges for practical deployment. To address these issues, knowledge distillation (KD) [15] has emerged as a key technique. KD involves transferring knowledge from a large, complex teacher model to a smaller, more efficient student model, thereby maintaining high performance while reducing resource demands. Most distillation methods for auto-regressive text generation models, including LLMs, employ metrics of probability distribution distance, such as Kullback-Leibler (KL) divergence [18] and reverse KL divergence [13], aiming to align the token-level probability distributions between the teacher and student models.

The distribution matching-based distillation methods can be viewed as behavior cloning on a decision-making problem from the perspective of imitation learning [21; 13; 2]. Based on this concept, early works based on the teacher-generated outputs [18] or a supervised dataset [27] can be viewed as an *off-policy* approach. Recent works further incorporate an *on-policy* approach, training the student on its self-generated outputs [21], using KL-based divergence [13; 2; 19] and total variation (TV) distance [35]. Accordingly, such distribution matching-based methods face the sub-optimality problem. The objective functions aimed at aligning the probability distributions between the teacher and student models can be straightforward but cannot fully capture the goal of distilling language knowledge. First, intuitively, the correct output for an input can vary, and thus behavior cloning cannot capture the full knowledge of a teacher. Besides, there is no standardized definition for the quality of a generated output given an input, which makes it difficult to define the objective of knowledge distillation. This

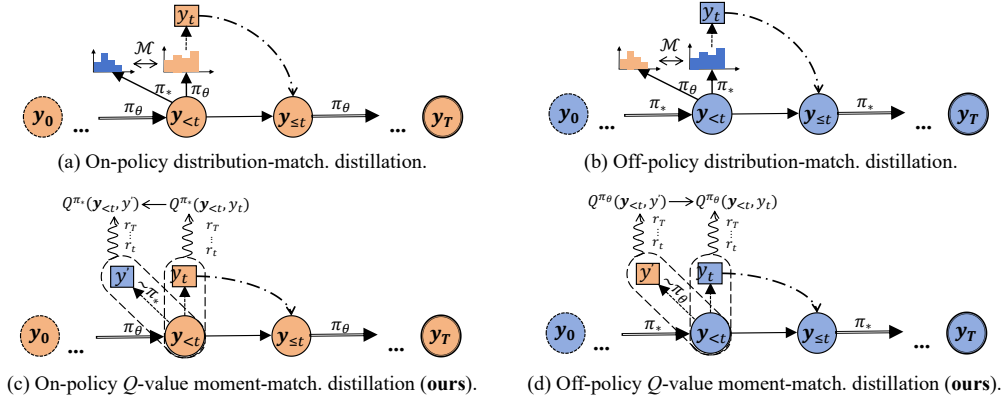


Figure 1: The comparison between the distribution-matching-based distillation and the action-value moment-matching distillation is outlined. π_θ and π_* denote the student policy and the teacher policy, respectively. For both on-policy (using student-generated outputs) and off-policy (using teacher-generated outputs) perspectives, our approach optimizes moment-matching of action-value functions (Q -functions) instead of minimizing the distribution distance measured by $\mathcal{M} = \text{KL}, \text{RKL}, \text{TV}$, etc.

imposes a significant limitation on the generalization performance of the student model through distillation.

To address the aforementioned issues, we employ a reinforcement learning (RL) formulation for the auto-regressive text generation problem and utilize the definition of imitation gap to describe the high-level goal of knowledge distillation. Additionally, we address the imitation gap for KD by matching moments of the action-value function, which reflects the quality of token-level predictions for the entire output. In addressing the action-value function, we adopt the approach of Swamy et al. [30], considering a two-player minimax game between the language policy and the action-value functions, aiming to minimize an upper bound of the moment-matching objective. For this purpose, we introduce an adversarial training algorithm based on the policy gradient to jointly optimize the on-/off-policy objectives. Figure 1 illustrates the overall approach.

We evaluate our approach on both the instruction-following dataset and three task-specific datasets for text summarization, machine translation, and commonsense reasoning. Results demonstrate that the proposed adversarial moment-matching approach effectively optimizes the moment-matching distance of the imitation gap and outperforms state-of-the-art KD methods and a range of distribution-matching-based methods. The code and implementation is released at <https://github.com/jiachenwestlake/MMKD>.

2 Related Work

Distillation of large language models. There has been an increasing interest in knowledge distillation (KD) of auto-regressive LMs, especially concerning large language models (LLMs) [37; 38]. This process effectively transfers elicited knowledge from teacher LLMs to smaller student models, aiming to compress the large size of neural network parameters and make LLMs more efficient. Sequence-level KD (SeqKD) [18] is a variation of supervised fine-tuning (SFT) in KD. It can be viewed as the simplest method for distillation of black-box LLMs by fine-tuning the student model with teacher-generated outputs. This method has been extensively used for LLMs and has achieved success [31; 5]. In contrast, distillation of white-box LLMs can make full use of internal information of the teacher model, such as logits [27; 35] and hidden states [20], for distribution alignment, making it more effective and efficient for KD. However, unlike previous work that explicitly clones the distribution of teacher LLMs into student models, this work learns an auxiliary Q -value function to guide KD.

Distillation via distribution matching. Most promising results in the distillation of white-box LLMs are achieved by minimizing divergence between the probability distributions of the teacher model and student models. Kullback-Leibler (KL) divergence, reverse Kullback-Leibler (RKL) divergence, and Jensen-Shannon (JS) divergence are three widely used KD objectives for auto-regressive LMs

[35; 13; 2; 19; 37]. Wen et al. [35] have shown the equivalent formulations of sequence-level KL, RKL, JS divergences, and the step-wise terms. Additionally, they also present the strong performance of step-wise total variation (TV) distance for KD, which can upper bound the sequence-level term. As a result, most recent works focus on on-policy approaches for KD [2] and combine the real-time-generated outputs by students (on-policy) with the real-time-generated outputs by teachers (or from supervised datasets) (off-policy). Following this line, Gu et al. [13] further propose a policy gradient-based method to address the high variance issues of RKL-based methods, while Ko et al. [19] propose a more efficient and effective method using a skew KL divergence loss and an adaptive off-policy approach. We also focus on a combination of on-policy and off-policy objectives for KD, but we introduce a more sophisticated moment-matching approach instead of directly using the well-studied distribution-matching metrics such as KL, RKL, JS divergences, and TV distance.

Distillation via reinforcement learning. In a common formulation of RL in text generation [40; 23; 14], an auto-regressive model can be viewed as a language policy, making decisions on the next token (action) based on the currently generated sequence (state). From this perspective, KD corresponds to behavior cloning in imitation learning [18; 6; 13; 2]. For imitation learning in text generation, early works such as SeqGAN [40] and TextGAIL [36] utilize a generative adversarial framework to balance between the reward model, optimized by discriminating generated/real-word text, and the language policy, optimized by policy gradient-based methods using the reward model. Existing work on KD via imitation learning refers to ImitKD [21], which optimizes the student policy by learning from demonstrations of the teacher model. RL-based distillation can also be especially relevant for leveraging the feedback from the teacher to train student models [3; 7], in which teacher models are used to generate the feedback data for training a reward model. We build our method upon a RL-based imitation learning framework. However, unlike previous work [18; 13; 2], we propose an adversarial moment-matching approach to enhance behavior cloning.

3 Method

3.1 Notations and Definitions

In this section, we consider the text generation task as a decision-making process and give a corresponding reinforcement learning (RL) formulation.

Text generation. Given an input \mathbf{x} , the auto-regressive generation task in our work aims to generate a sequence of tokens as the output (y_1, \dots, y_T) , where y_t comes from a vocabulary \mathcal{V} . For simplicity, we define $\mathbf{y} = (y_0, y_1, \dots, y_T)$ as the full input-output sequence, where $y_0 = \mathbf{x}$. The generator is modeled by a conditional probability distribution $p_\theta(\mathbf{y}|\mathbf{x}) = \prod_{t=1}^T p_\theta(y_t|\mathbf{y}_{<t})$, where $\mathbf{y}_{<t}$ denotes the prefix $(y_0, y_1, \dots, y_{t-1})$.

RL formulation. We formulate text generation as a sequential decision-making process. At each time step $t \in \{1, \dots, T\}$, the policy π_θ takes an action $y_t \in \mathcal{V}$ based on the current state $\mathbf{y}_{<t} \in \mathcal{Y}$, transits to the next state $\mathbf{y}_{<t+1} \in \mathcal{Y}^1$ and receives a reward $r(\mathbf{y}_{<t}, y_t)$ by a reward function $r : \mathcal{Y} \times \mathcal{V} \rightarrow \mathbb{R}$. The policy corresponds to the generation model $\pi_\theta(y_t|\mathbf{y}_{<t}) = p_\theta(y_t|\mathbf{y}_{<t})$. A trajectory $\tau \sim \pi_\theta = \{\mathbf{y}_{<t}, y_t\}_{t=1, \dots, T}$ refers to a sequence of state-action pairs generated by first sampling a state $y_0 = \mathbf{x}$ from $p_\mathbf{x}$ and then repeatedly sampling an action y_t from $\pi_\theta(\cdot|\mathbf{y}_{<t})$ and obtain the next state $\mathbf{y}_{<t+1}$ for T time steps. We also define our value function and Q -value function as $V^{\pi_\theta}(\mathbf{y}_{<t}) = \mathbb{E}_{\tau \sim \pi_\theta|\mathbf{y}_{<t}} \sum_{t'=t}^T r(\mathbf{y}_{<t'}, y_{t'})$ and $Q^{\pi_\theta}(\mathbf{y}_{<t}, y_t) = \mathbb{E}_{\tau \sim \pi_\theta|\mathbf{y}_{<t}, y_t} \sum_{t'=t}^T r(\mathbf{y}_{<t'}, y_{t'})$. We define the RL objective in our generation task to maximize the performance $J(\pi_\theta) = \mathbb{E}_{\tau \sim \pi_\theta} \left[\sum_{t=1}^T r(\mathbf{y}_{<t}, y_t) \right]$.

3.2 Knowledge Distillation as Moment-Matching Imitation Learning

Based on the RL formulation of auto-regressive generation, we can view the goal of knowledge distillation at a high-level as to bridge the performance gap between the teacher policy and the student policy.

¹In text generation, the state-transition is commonly assumed to be deterministic [40; 23], i.e., $p(\mathbf{y}_{<t+1}|\mathbf{y}_{<t}, y_t) = 1$.

Definition 1 (Imitation gap). We define the imitation gap between the teacher policy and student policy as:

$$J(\pi_*) - J(\pi_\theta) = \mathbb{E}_{\tau \sim \pi_*} \left[\sum_{t=1}^T r(\mathbf{y}_{<t}, y_t) \right] - \mathbb{E}_{\tau' \sim \pi_\theta} \left[\sum_{t=1}^T r(\mathbf{y}'_{<t}, y'_t) \right], \quad (1)$$

where $\tau \sim \pi_* = \{\mathbf{y}_{<t}, y_t\}_{t=1, \dots, T}$ denotes the trajectory of teacher policy and $\tau' \sim \pi_\theta = \{\mathbf{y}'_{<t}, y'_t\}_{t=1, \dots, T}$ denotes the trajectory of student policy.

From the perspective of imitation learning [30; 29], the objective of distillation from the teacher policy π_* to the student policy π_θ can be represented as to minimize the imitation gap of Eq. (1) w.r.t. the parameters of student policy θ . An direct idea from Eq. (1) is to use moment matching over the reward to optimize the imitation gap [30]. However, we actually care about the long-term reward, at each time step, we should consider the accumulated reward in the future output rather than the immediate reward to the fitness of previous tokens (prefix). To this end, we can alternatively use the Q -value function (def. in Sec. 3.1) for each timestep to represent the overall reward from the current timestep to the last timestep. Similar to [30], we can apply the Performance Difference Lemma (PDL) to expand the imitation gap in Eq. (1) into either off-policy or on-policy expressions.

Proposition 1 (Off-policy bound of imitation gap). Let \mathcal{F}_Q denote the set of Q -value functions induced by sampling actions from π_θ , then we have:

$$J(\pi_*) - J(\pi_\theta) \leq \sup_{f \in \mathcal{F}_Q} \mathbb{E}_{\substack{\mathbf{x} \sim p_{\mathbf{x}} \\ \tau \sim \pi_* | \mathbf{y}_0 = \mathbf{x}}} \underbrace{\left[\sum_{t=1}^T \left(f(\mathbf{y}_{<t}, y_t) - \mathbb{E}_{y \sim \pi_\theta(\cdot | \mathbf{y}_{<t})} [f(\mathbf{y}_{<t}, y)] \right) \right]}_{\mathcal{U}^{\text{off}}(\tau, f, \theta)} \quad (2)$$

In the following sections, we will use $\mathcal{U}^{\text{off}}(\tau, f, \theta)$ to represent a sampled off-policy imitation gap with an trajectory $\tau \sim \pi_* | \mathbf{y}_0 = \mathbf{x}$ w.r.t. a Q -value function f and a teacher policy π_θ .

Proof. The derivation is mostly followed Swamy et al. [30]. See Appendix A.1 for the complete derivation. \square

The off-policy upper bound of the imitation gap in Proposition 1 only requires a collected dataset of teacher-generated trajectories to be evaluated and minimized.

Proposition 2 (On-policy bound of imitation gap). Let \mathcal{F}_{Q_*} denote the set of Q functions induced by sampling actions from π_* , then we have:

$$J(\pi_*) - J(\pi_\theta) \leq \sup_{f \in \mathcal{F}_{Q_*}} \mathbb{E}_{\substack{\mathbf{x} \sim p_{\mathbf{x}} \\ \tau \sim \pi_\theta | \mathbf{y}_0 = \mathbf{x}}} \underbrace{\left[\sum_{t=1}^T \left(\mathbb{E}_{y \sim \pi_*(\cdot | \mathbf{y}_{<t})} [f(\mathbf{y}_{<t}, y)] - f(\mathbf{y}_{<t}, y_t) \right) \right]}_{\mathcal{U}^{\text{on}}(\tau, f)} \quad (3)$$

In the following sections, we will use $\mathcal{U}^{\text{on}}(\tau, f)$ to represent a sampled on-policy imitation gap with an trajectory $\tau \sim \pi_\theta | \mathbf{y}_0 = \mathbf{x}$ w.r.t. a Q -value function f given the teacher policy π_* .

Proof. The derivation is mostly followed Swamy et al. [30]. See Appendix A.2 for the complete derivation. \square

It is notable from Proposition 2 that the on-policy upper bound of the imitation gap requires interactions with the teacher to tell us what action they would take in any state visited by the student as well as on-policy samples from the student's current policy $\tau \sim \pi_\theta$.

In the remaining content of this section, we will exploring the relationship between the proposed upper bounds of the imitation gap and the existing distribution-matching objectives [35]. At the beginning, we draw a general formulation of the state-of-the-art methods for distillation of LLMs [35; 13; 2; 19] that rely on distribution-matching between the student's and teacher's predictions, through minimizing the step-wise probability distribution distance between the teacher policy and student policy.

Definition 2 (Generalized step-wise distribution distance). *The off-policy and on-policy versions are defined as follows,*

$$d_{\mathcal{M}}^{\text{off}}(\pi_{\theta}, \pi_{*}) := \mathbb{E}_{\substack{\varpi \sim p_{\varpi} \\ \tau \sim \pi_{*} | \mathbf{y}_0 = \varpi}} \left[\sum_{t=1}^T \mathcal{M}(\pi_{*}(\cdot | \mathbf{y}_{<t}), \pi_{\theta}(\cdot | \mathbf{y}_{<t})) \right]; \quad (4)$$

$$d_{\mathcal{M}}^{\text{on}}(\pi_{\theta}, \pi_{*}) := \mathbb{E}_{\substack{\varpi \sim p_{\varpi} \\ \tau \sim \pi_{\theta} | \mathbf{y}_0 = \varpi}} \left[\sum_{t=1}^T \mathcal{M}(\pi_{*}(\cdot | \mathbf{y}_{<t}), \pi_{\theta}(\cdot | \mathbf{y}_{<t})) \right], \quad (5)$$

where $\mathcal{M}(\cdot, \cdot)$ denotes a distribution distance, consisting of total variation (TV) distance [35] and Kullback-Leibler (KL)-based divergence [13; 2]. Detailed definitions for these distances refer to Appendix A.3.

It is notable from Wen et al. [35] that the sequence-level KL, RKL and JS divergences can be equivalently represented as the step-wise terms, and the sequence-level TV distance can be upper bounded by the step-wise terms, which can be actually implemented by algorithms. To make a connection with the step-wise distribution distance (Definition 2), we use the following definition.

Definition 3 (Distribution-matching formulation of moment-matching bounds). *Based on Definition 2, we can re-formulate the on-policy and off-policy moment-matching (MM) bounds (Proposition 2 and Proposition 1, respectively) via step-wise distribution-matching, which can be defined as $d_{\text{MM}}^{\text{on}}(\pi_{\theta}, \pi_{*})$ and $d_{\text{MM}}^{\text{off}}(\pi_{\theta}, \pi_{*})$ respectively, where the distance metric $\text{MM}(\cdot, \cdot)$ can be defined as follows,*

$$\begin{aligned} \text{MM}(\pi_{*}(\cdot | \mathbf{y}_{<t}), \pi_{\theta}(\cdot | \mathbf{y}_{<t})) &= \mathbb{E}_{y \sim \pi_{*}(\cdot | \mathbf{y}_{<t})} [f_{*}(\mathbf{y}_{<t}, y)] - \mathbb{E}_{y' \sim \pi_{\theta}(\cdot | \mathbf{y}_{<t})} [f_{*}(\mathbf{y}_{<t}, y')], \\ \text{Off-policy: } f_{*} &= \arg \max_{f \in \mathcal{F}_{Q_{*}}} \mathbb{E}_{\substack{\varpi \sim p_{\varpi} \\ \tau \sim \pi_{*} | \mathbf{y}_0 = \varpi}} [\mathcal{U}^{\text{off}}(\tau, f, \theta)]; \\ \text{On-policy: } f_{*} &= \arg \max_{f \in \mathcal{F}_Q} \mathbb{E}_{\substack{\varpi \sim p_{\varpi} \\ \tau \sim \pi_{\theta} | \mathbf{y}_0 = \varpi}} [\mathcal{U}^{\text{on}}(\tau, f)] \end{aligned} \quad (6)$$

Under Definition 3, we observe that the main difference between the moment-matching bounds and other step-wise distribution distance, e.g., TV distance and KL-based divergences in formulation comes from the optimal Q -value function f_{*} , aiming to maximize the discrepancy of its expectations based on $\pi_{*}(\cdot | \mathbf{y}_{<t})$ v.s. $\pi_{\theta}(\cdot | \mathbf{y}_{<t})$ for each step $t \in \{1, 2, \dots, T\}$. To look deeper, we draw a connection between moment-matching bounds and the step-wise TV distance using the following corollary.

Corollary 1. *Under a constrain on the class of Q -value functions: $\mathcal{F}_{Q_{\theta}} = \mathcal{F}_{Q_{*}} = \{f : \|f\|_{\infty} \leq 1\}$, the moment-matching bounds in Proposition 1 and Proposition 2 can be upper-bounded by the step-wise TV distance in Definition 2, Formally, for the off-policy and on-policy perspectives, we have:*

$$J(\pi_{*}) - J(\pi_{\theta}) \leq \sup_{f: \|f\|_{\infty} \leq 1} \mathbb{E}_{\substack{\varpi \sim p_{\varpi} \\ \tau \sim \pi_{*} | \mathbf{y}_0 = \varpi}} [\mathcal{U}^{\text{off}}(\tau, f, \theta)] \leq d_{\text{TV}}^{\text{off}}(\pi_{\theta}, \pi_{*}); \quad (7)$$

$$J(\pi_{*}) - J(\pi_{\theta}) \leq \sup_{f: \|f\|_{\infty} \leq 1} \mathbb{E}_{\substack{\varpi \sim p_{\varpi} \\ \tau \sim \pi_{\theta} | \mathbf{y}_0 = \varpi}} [\mathcal{U}^{\text{on}}(\tau, f)] \leq d_{\text{TV}}^{\text{on}}(\pi_{\theta}, \pi_{*}) \quad (8)$$

Proof. See Appendix A.4 for the complete derivation. □

We can observe from Corollary 1 that minimizing the step-wise TV distance can achieve sub-optimal results for the moment-matching bounds. Optimizing the moment-matching bounds can potentially achieve better optimization results for imitation learning objectives.

3.3 Adversarial Training Algorithm

Optimization objective. As shown in previous work [13; 2; 19] that incorporating both the on-policy and off-policy distillation benefits effectiveness and efficiency. We thus consider a training objective to jointly minimize the on-policy upper bound of Proposition (2) and the off-policy upper bound of Proposition (1). Both the moment-matching objectives can be optimized by viewing the learning

Algorithm 1: Adversarial training procedure

Input: Dataset \mathcal{D}_{xy} with inputs and ground-truth outputs;

Teacher policy π_* , student policy π_θ with initial parameters θ pretrained on \mathcal{D}_{xy} , off-policy Q -value function f_{ϕ_1} , on-policy Q -value function f_{ϕ_2} ;

Learning rate η , batch size M , control factor α

Output: A optimized student policy π_θ

while θ has not converged **do**

for $k = 0, 1, 2, \dots, K$ **do**

 Sample an input $\mathbf{x} \sim \mathcal{D}_{\mathbf{x}}$ and generate an output trajectory $\tau_{\text{off}} \sim \pi_* | \mathbf{y}_0 = \mathbf{x}$

$\phi_1 \leftarrow \phi_1 + \alpha \eta \nabla_{\phi_1} \mathcal{U}^{\text{off}}(\tau_{\text{off}}, f_{\phi_1}, \theta)$ \triangleright maximize $\mathcal{L}(\theta, \phi_1, \phi_2)$ by Eq. (11)

 Sample an input $\mathbf{x} \sim \mathcal{D}_{\mathbf{x}}$ and generate an output trajectory $\tau_{\text{on}} \sim \pi_\theta | \mathbf{y}_0 = \mathbf{x}$

$\phi_2 \leftarrow \phi_2 + \alpha \eta \nabla_{\phi_2} \mathcal{U}^{\text{on}}(\tau_{\text{on}}, f_{\phi_2})$ \triangleright maximize $\mathcal{L}(\theta, \phi_1, \phi_2)$ by Eq. (12)

end

 Sample an input $\mathbf{x} \sim \mathcal{D}_{\mathbf{x}}$ and generate output trajectories $\tau_{\text{off}} \sim \pi_* | \mathbf{y}_0 = \mathbf{x}$ and $\tau_{\text{on}} \sim \pi_\theta | \mathbf{y}_0 = \mathbf{x}$

$\theta \leftarrow \theta - \eta (\mathcal{G}_{\text{on}}(\tau_{\text{on}}, \theta) - \mathcal{G}_{\text{off}}(\tau_{\text{off}}, \theta))$ \triangleright minimize $\mathcal{L}(\theta, \phi_1, \phi_2)$ by Eq. (10)

end

procedure as solving a game. More specifically, we consider a two-player minimax game between the student policy and the Q -value functions. To this end, we consider using parameter estimation methods for the Q -value functions and assume that both \mathcal{F}_Q and \mathcal{F}_{Q_*} can be represented using a parameterized class of functions $\{f_\phi\}_{\phi \in \Phi}$, wherein we use ϕ_1 and ϕ_2 to denote parameters of the off-policy and on-policy Q -value functions, respectively. Thereby, the learning problem can be represented as follows,

$$\min_{\theta \in \Theta} \max_{\phi_1, \phi_2 \in \Phi} \underbrace{\mathbb{E}_{\mathbf{x} \sim p_{\mathbf{x}}} \left[\mathbb{E}_{\tau \sim \pi_* | \mathbf{y}_0 = \mathbf{x}} [\mathcal{U}^{\text{off}}(\tau, f_{\phi_1}, \theta)] + \mathbb{E}_{\tau' \sim \pi_\theta | \mathbf{y}_0 = \mathbf{x}} [\mathcal{U}^{\text{on}}(\tau', f_{\phi_2})] \right]}_{\mathcal{L}(\theta, \phi_1, \phi_2) :=} \quad (9)$$

We denote the learning objective by $\mathcal{L}(\theta, \phi_1, \phi_2)$. To minimize the objective of $\mathcal{L}(\theta, \phi_1, \phi_2)$ w.r.t the policy parameters θ , we use a policy gradient-based approach and derive the policy gradient of $\mathcal{L}(\theta)$ w.r.t θ in Appendix A.5, represented as follows,

$$\begin{aligned} \nabla_{\theta} \mathcal{L}(\theta, \phi_1, \phi_2) &= \mathbb{E}_{\mathbf{x} \sim p_{\mathbf{x}}} \left[- \mathbb{E}_{\tau \sim \pi_* | \mathbf{y}_0 = \mathbf{x}} [\mathcal{G}_{\text{off}}(\tau, \theta)] + \mathbb{E}_{\tau' \sim \pi_\theta | \mathbf{y}'_0 = \mathbf{x}} [\mathcal{G}_{\text{on}}(\tau', \theta)] \right] \\ \text{s.t. } \mathcal{G}_{\text{off}}(\tau, \theta) &= \sum_{t=1}^T \mathbb{E}_{y' \sim \pi_\theta(\cdot | \mathbf{y}_{<t})} \nabla_{\theta} \log \pi_\theta(y' | \mathbf{y}_{<t}) f_{\phi_1}(\mathbf{y}_{<t}, y'); \\ \mathcal{G}_{\text{on}}(\tau', \theta) &= \sum_{t=1}^T \nabla_{\theta} \log \pi_\theta(y'_t | \mathbf{y}'_{<t}) \mathcal{U}^{\text{on}}(\tau', f_{\phi_2}) \end{aligned} \quad (10)$$

Besides, to maximize the objective of $\mathcal{L}(\theta, \phi_1, \phi_2)$ w.r.t. parameters of the on-policy Q -value function ϕ_1 and parameters of the off-policy Q -value function ϕ_2 , we use a stochastic gradient ascent method and represent the corresponding gradients as follows,

$$\nabla_{\phi_1} \mathcal{L}(\theta, \phi_1, \phi_2) = \mathbb{E}_{\tau \sim \pi_* | \mathbf{y}_0 = \mathbf{x}} [\nabla_{\phi_1} \mathcal{U}^{\text{off}}(\tau, f_{\phi_1}, \theta)] \quad (11)$$

$$\nabla_{\phi_2} \mathcal{L}(\theta, \phi_1, \phi_2) = \mathbb{E}_{\tau' \sim \pi_\theta | \mathbf{y}_0 = \mathbf{x}} [\nabla_{\phi_2} \mathcal{U}^{\text{on}}(\tau', f_{\phi_2})] \quad (12)$$

Training procedure. The training objective is to achieve a Nash equilibrium between the parameters of student policy θ and the parameters of on-policy and off-policy Q -value functions ϕ_1, ϕ_2 for the optimization problem of $\min_{\theta} \max_{\phi_1, \phi_2} \mathcal{L}(\theta, \phi_1, \phi_2)$ in Eq. (9). To this end, we use an adversarial training strategy in Algorithm 1, by starting from a student model fine-tuned on a dataset \mathcal{D}_{xy} . In the training algorithm, we iteratively maximize the objective w.r.t. the parameters of Q -value functions ϕ_1, ϕ_2 and simultaneously minimize the objective w.r.t. the parameters of student policy θ . In each iteration of policy updating, we first perform K steps of gradient ascent w.r.t. the parameters of Q -value functions ϕ_1, ϕ_2 , where the gradients in Eq. (11) and Eq. (12) are approximately computed

Method	DollyEval		SelfInst		VicunaEval		S-NI	UnNI
	GPT4	R-L	GPT4	R-L	GPT4	R-L	R-L	R-L
<i>OpenLLaMA2-7B (teacher)</i>	58.8 \pm 1.2	32.5 \pm 0.4	56.7 \pm 0.8	21.6 \pm 0.2	46.2 \pm 0.6	22.6 \pm 0.5	36.3 \pm 0.5	38.5 \pm 0.2
SFT (student)	46.8 \pm 0.7	26.7 \pm 0.6	40.8 \pm 1.1	16.3 \pm 0.7	34.8 \pm 0.8	17.3 \pm 0.2	30.4 \pm 0.4	28.6 \pm 0.3
KD [15]	43.9 \pm 0.8	22.4 \pm 0.4	43.5 \pm 0.5	17.4 \pm 0.5	33.7 \pm 0.3	16.4 \pm 0.2	29.3 \pm 0.6	23.4 \pm 0.3
SeqKD [18]	50.2 \pm 0.6	26.2 \pm 0.4	46.8 \pm 0.3	15.8 \pm 0.5	38.8 \pm 1.2	18.0 \pm 0.6	29.7 \pm 0.3	27.8 \pm 0.1
ImitKD [21]	53.7 \pm 1.6	25.3 \pm 0.3	45.0 \pm 0.7	18.4 \pm 0.4	41.7 \pm 1.2	19.1 \pm 0.2	33.1 \pm 0.7	28.7 \pm 0.5
MiniLLM [13]	58.7 \pm 1.2	28.4 \pm 0.3	51.8 \pm 1.5	20.2 \pm 0.6	44.2 \pm 1.1	20.7 \pm 0.5	37.4 \pm 0.4	37.5 \pm 0.2
GKD [2]	57.6 \pm 1.0	27.5 \pm 0.3	52.4 \pm 1.2	20.9 \pm 0.3	45.5 \pm 0.8	19.3 \pm 0.5	36.8 \pm 0.6	34.8 \pm 0.3
DistiLLM [19]	59.2 \pm 1.2	29.5 \pm 0.2	53.4 \pm 1.0	20.8 \pm 0.7	46.3 \pm 0.9	20.4 \pm 0.3	37.2 \pm 0.1	38.2 \pm 0.1
ours	59.8\pm0.8	30.7\pm0.4	54.2\pm1.2	21.7\pm0.5	47.8\pm0.7	21.4\pm0.4	38.7\pm0.4	39.1\pm0.3

Table 1: Comparison with state-of-the-art KD methods on the instruction-following dataset using fine-tuned OpenLLaMA-7B as the teacher and fine-tuned OpenLLaMA-3B as the student. We format **the best**, the second best and worse than SFT results. The results based on GPT-2 are available in Appendix C.1.

by sampling inputs from the dataset and sampling the trajectories from the policies. Then, the parameters of student policy θ are updated by gradient descent with the estimated gradient of Eq. (11) with sampling inputs and policies.

4 Experiments

We consider task-agnostic instruction-following experiments and task-specific experiments, including text summarization, machine translation, and commonsense reasoning. We compare our approach with various KD baselines, including: SFT, which fine-tunes the student model on the supervised dataset \mathcal{D}_{xy} ; KD [15], which uses KL divergence on the supervised dataset \mathcal{D}_{xy} ; SeqKD [18], which applies SFT to the student model with teacher-generated outputs; ImitKD [21], which uses KL divergence on the student-generated outputs; MiniLLM [13], which uses RKL divergence with a policy gradient method; GKD [2], which uses JS divergence with an on-policy method; and DistiLLM [19], which uses an adaptive training method for off-policy optimization of a skew KL divergence. Additionally, we focus on step-wise distance optimization for KD and compare it with a range of well-known methods, including KL divergence, RKL divergence, JS divergence, and TV distance, as discussed by Wen et al. [35]. All the reported results are the average across three random seeds.

4.1 Task-Agnostic Distillation

Experimental Setup. We follow the previous works [13; 19] for the implementation of the instruction-following experiment, aiming to evaluate the distilled model’s ability to handle diverse tasks presented in the form of instructions. We construct the training data from `databricks-dolly-15k` [8], where we randomly select 15K samples for training and equally split 500 samples for validation and testing. We evaluate the trained model on five instruction-following datasets: DollyEval, SelfInst [33], VicunaEval [5], S-NI [34], and UnNI [16]. Following the previous works [13; 19], we also add the OpenWebText [12] corpus, consisting of long-document plain text, for joint training with a language modeling task. This has been shown to effectively improve the performance of instruction tuning [13]. The evaluation metrics include ROUGE-L [22] and GPT-4 feedback with the same prompts as in [19]. More details on experimental setup refer to Appendix B.

Main results. Table 1 illustrates the instruction-following performances. Compared with the SFT baseline, which indicates the student model without KD, KD and SeqKD hardly improve the performances. This indicates that using only supervised datasets or teacher-generated outputs does not benefit the KD of large language models. In contrast, utilizing the student-generated outputs with KL divergence [2], RKL divergence [13], and JS divergence [2] shows effectiveness for KD in the instruction-following task. State-of-the-art methods [13; 2; 19] tend to combine the student-generated outputs with the teacher-generated output or supervised dataset to further improve the results of KD. This shows that a mixture optimization of both on-policy and off-policy objectives can effectively improve the KD performance of large language models on the instruction-following task. In particular, we use an adversarial moment-matching method and optimize both on-policy and off-policy objectives for KD, thus achieving the best results on five test datasets with both GPT4 feedback and ROUGE-L evaluations.

Method	SAMSum			IWSLT'17 (en-de)			StrategyQA		
	T5-Small	T5-Base	T5-Large	T5-Small	T5-Base	T5-Large	T5-Small	T5-Base	T5-Large
<i>T5-XL (teacher)</i>	52.5±0.4			35.2±0.2			64.5±0.8		
SFT (student)	40.6±0.2	47.3±0.3	49.8±0.2	21.5±0.1	30.1±0.0	33.7±0.1	52.4±0.5	57.5±0.8	60.7±0.8
KD [15]	39.2±0.4	46.5±0.3	47.4±0.3	21.7±0.1	29.8±0.2	31.7±0.1	49.7±0.3	55.3±0.1	59.2±0.5
SeqKD [18]	39.7±0.3	47.7±0.5	49.3±0.4	21.2±0.3	29.2±0.2	32.9±0.5	50.6±0.7	57.5±1.1	61.5±0.8
ImitKD [21]	41.8±0.3	48.6±0.7	51.2±0.5	22.2±0.3	28.7±0.6	34.1±0.2	53.8±0.8	59.7±0.5	61.7±0.6
GKD [2]	42.1±0.3	48.2±0.5	51.7±0.4	22.7±0.2	31.2±0.1	34.7±0.2	55.6±0.4	60.3±0.5	63.6±0.3
DistiLLM [19]	42.6±0.2	49.4±0.6	52.1±0.4	22.5±0.1	30.8±0.2	35.5±0.1	56.3±0.3	61.2±0.7	62.8±0.2
ours	43.7±0.4	50.4±0.3	52.7±0.3	23.7±0.1	32.4±0.3	36.0±0.2	58.2±0.4	62.9±0.3	65.3±0.7

Table 2: Comparison with the state-of-the-art KD methods on text summarization, machine translation and commonsense reasoning datasets. We report the ROUGE-L, BLEU and accuracy for SAMSum, IWSLT'17 (en-de) and StrategyQA, respectively. We format **the best**, the second best and worse than SFT results.

4.2 Task-Specific Distillation

Experimental Setup. We evaluated the KD models on three tasks consisting of text summarization, machine translation, and reasoning. For the text summarization task, we follow Ko et al. [19] to conduct experiments on the SAMSum [11] dataset. For the machine translation tasks, we follow Ko et al. [19] to conduct experiments on the IWSLT'17 (en-de) [4] dataset. For the commonsense reasoning task, we conduct experiments on the StrategyQA dataset [10]. For all of the task-specific experiments, we use T5-XL [26] as the teacher model and T5-Large/-Base/-Small as the student models. For the machine translation experiments, we employ a multilingual pretrained model, mT5 [39], to build the methods. For evaluation, we use ROUGE-L [22], BLEU [24], and accuracy as the performance metrics on SAMSum, IWSLT'17 (en-de), and StrategyQA, respectively. More details about the experimental setup refer to Appendix B.

Main results. Table 2 displays the performances on three task-specific datasets. Since the original work of MiniLLM [13] does not consider these tasks, we thus do not make comparisons with MiniLLM. The performance trend is similar to the instruct-following results, revealing that KD of large language models for specific tasks also benefits from the combination of on-policy objectives with student-generated outputs and off-policy objectives with teacher-generated outputs or supervised datasets. Additionally, we observe that student models of different sizes all benefit from the KD methods to improve performance. Overall, our approach achieves the best results on all three task-specific datasets for student models of different sizes. This demonstrates the effectiveness of an adversarial moment-matching approach for KD of large language models on specific tasks.

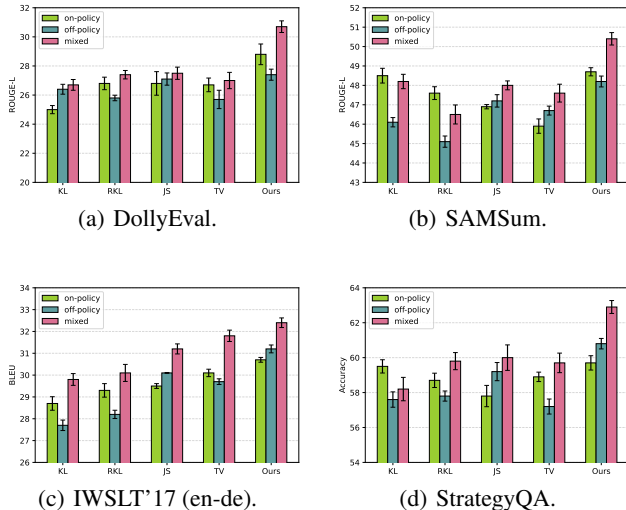


Figure 2: Performance of difference step-wise distribution distances.

4.3 Analysis on Step-Wise Distance Optimization

Comparison with distribution matching. We make comparisons with different step-wise distribution distances with a uniform formulation of Definition 2, considering the on-policy, off-policy objectives as well as the joint form. Results on four tasks are shown in Figure 2, more instruct-following results are available in Appendix C.2. Compared with the KL divergence, RKL divergence, JS divergence and total variation distance, the proposed moment-matching distance achieves the best

results under both the on-policy and off-policy training objectives, which shows that the proposed moment-matching approach is effective for KD of large language models. Besides, we observe that using a joint objective of both on-policy and off-policy can further significantly improve the performances. This shows that both on-policy and off-policy moment-matching objectives contribute to the minimization of the imitation gap and can thus benefit the KD of large language models.

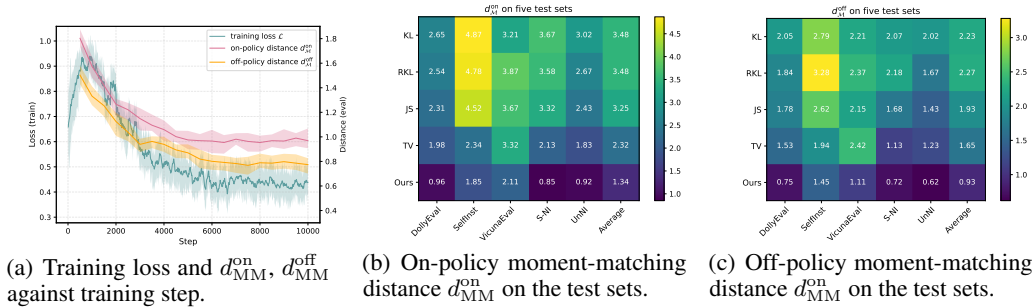


Figure 3: Adversarial training procedure for optimizing the on-policy and off-policy moment-matching distances d_{MM}^{on} , d_{MM}^{off} on the instruction-following dataset.

Adversarial training procedure. We present the training loss and moment-matching distance against the adversarial training steps. As depicted in Figure 3 (a), the training loss initially increases within the first 0-1,000 steps, indicating that initially, the Q -value functions are stronger than the policy in maximizing the loss function $\mathcal{L}(\theta, \phi_1, \phi_2)$ in Eq. (9). Concurrently, the policy gradient method contributes to minimizing the training loss, which eventually converges to a much lower stable value. Additionally, both the on-policy and off-policy moment-matching distances d_{MM}^{on} and d_{MM}^{off} decrease and eventually reach a low value with only minor fluctuations. For more results and details on experimental setups, please refer to Appendix C.3.

Moment-matching distance optimization. We further illustrate the on-policy moment-matching distance d_{MM}^{on} and the off-policy moment-matching distance d_{MM}^{off} (defined in Definition 3) optimized by different step-wise distances in Figure 3 (b) and (c), respectively. Interestingly, we observe that the total variation (TV) distance obtains the second-best results on average for both on-policy and off-policy distances. This finding suggests a similarity between the formulations of TV distance and moment-matching distances to some extent, as supported by the theoretical result of Corollary 1. Across all instruction-following test sets, our approach effectively optimizes both on-policy and off-policy moment-matching distances more than other step-wise distribution distances used in KD, including KL divergence, RKL divergence, JS divergence, and TV distance. This observation also underscores the effectiveness of our policy gradient methods. Extensive results on the task-specific datasets are available in Appendix C.4.

5 Conclusion

In this work, we investigated a moment-matching approach for knowledge distillation of large language models. Specifically, we formulated knowledge distillation from a perspective of imitation learning and derived both on-policy and off-policy bounds for the imitation gap between the teacher model and student model via moment-matching distance. Additionally, we proposed an adversarial training algorithm to simultaneously estimate and minimize the joint objective of on-policy and off-policy moment-matching distances. In experiments, we evaluated the proposed algorithm on four instruction-following datasets and three task-specific datasets, comparing it with a range of state-of-the-art KD methods as well as four well-studied step-wise distribution distances for KD of auto-regressive models. Results demonstrate that our approach can effectively leverage the policy gradient method to optimize the moment-matching distance and achieve the best results across all datasets.

Limitations and future work. The proposed adversarial training algorithm requires additional computational steps for the inner-loop gradient ascent, which may result in increased time complexity. Moreover, the proposed approach necessitates auxiliary networks to build the Q -value functions, which may incur additional memory costs. Therefore, in future work, we aim to enhance the time and memory efficiency of our approach.

References

- [1] Josh Achiam, Steven Adler, Sandhini Agarwal, Lama Ahmad, Ilge Akkaya, Florencia Leoni Aleman, Diogo Almeida, Janko Altenschmidt, Sam Altman, Shyamal Anadkat, et al. Gpt-4 technical report. *arXiv preprint arXiv:2303.08774*, 2023.
- [2] Rishabh Agarwal, Nino Vieillard, Yongchao Zhou, Piotr Stanczyk, Sabela Ramos Garea, Matthieu Geist, and Olivier Bachem. On-policy distillation of language models: Learning from self-generated mistakes. In *The Twelfth International Conference on Learning Representations*, 2024.
- [3] Yuntao Bai, Saurav Kadavath, Sandipan Kundu, Amanda Askell, Jackson Kernion, Andy Jones, Anna Chen, Anna Goldie, Azalia Mirhoseini, Cameron McKinnon, et al. Constitutional ai: Harmlessness from ai feedback. *arXiv preprint arXiv:2212.08073*, 2022.
- [4] Mauro Cettolo, Marcello Federico, Luisa Bentivogli, Jan Niehues, Sebastian Stüker, Katsutho Sudoh, Koichiro Yoshino, and Christian Federmann. Overview of the iwslt 2017 evaluation campaign. In *Proceedings of the 14th International Workshop on Spoken Language Translation*, pages 2–14, 2017.
- [5] Wei-Lin Chiang, Zhuohan Li, Zi Lin, Ying Sheng, Zhanghao Wu, Hao Zhang, Lianmin Zheng, Siyuan Zhuang, Yonghao Zhuang, Joseph E Gonzalez, et al. Vicuna: An open-source chatbot impressing gpt-4 with 90%* chatgpt quality. See <https://vicuna.lmsys.org> (accessed 14 April 2023), 2(3):6, 2023.
- [6] Kamil Ciosek. Imitation learning by reinforcement learning. In *International Conference on Learning Representations*, 2021.
- [7] Ganqu Cui, Lifan Yuan, Ning Ding, Guanming Yao, Wei Zhu, Yuan Ni, Guotong Xie, Zhiyuan Liu, and Maosong Sun. Ultrafeedback: Boosting language models with high-quality feedback. *arXiv preprint arXiv:2310.01377*, 2023.
- [8] Free Dolly. Introducing the world’s first truly open instruction-tuned llm. databricks.com, 2023.
- [9] Xinyang Geng and Hao Liu. Openllama: An open reproduction of llama. URL: https://github.com/openlm-research/open_llama, 2023.
- [10] Mor Geva, Daniel Khashabi, Elad Segal, Tushar Khot, Dan Roth, and Jonathan Berant. Did aristotle use a laptop? a question answering benchmark with implicit reasoning strategies. *Transactions of the Association for Computational Linguistics*, 9:346–361, 2021.
- [11] Bogdan Gliwa, Iwona Mochol, Maciej Biesek, and Aleksander Wawer. Samsun corpus: A human-annotated dialogue dataset for abstractive summarization. *arXiv preprint arXiv:1911.12237*, 2019.
- [12] Aaron Gokaslan, Vanya Aaron, Ellie Pavlick, and Stefanie Tellex. Openwebtext corpus. 2019.
- [13] Yuxian Gu, Li Dong, Furu Wei, and Minlie Huang. Minillm: Knowledge distillation of large language models. In *The Twelfth International Conference on Learning Representations*, 2024.
- [14] Yongchang Hao, Yuxin Liu, and Lili Mou. Teacher forcing recovers reward functions for text generation. *Advances in Neural Information Processing Systems*, 35:12594–12607, 2022.
- [15] Geoffrey Hinton, Oriol Vinyals, and Jeff Dean. Distilling the knowledge in a neural network. *arXiv preprint arXiv:1503.02531*, 2015.
- [16] Or Honovich, Thomas Scialom, Omer Levy, and Timo Schick. Unnatural instructions: Tuning language models with (almost) no human labor. *arXiv preprint arXiv:2212.09689*, 2022.
- [17] Jared Kaplan, Sam McCandlish, Tom Henighan, Tom B Brown, Benjamin Chess, Rewon Child, Scott Gray, Alec Radford, Jeffrey Wu, and Dario Amodei. Scaling laws for neural language models. *arXiv preprint arXiv:2001.08361*, 2020.

- [18] Yoon Kim and Alexander M Rush. Sequence-level knowledge distillation. In *Proceedings of the 2016 Conference on Empirical Methods in Natural Language Processing*. Association for Computational Linguistics, 2016.
- [19] Jongwoo Ko, Sungnyun Kim, Tianyi Chen, and Se-Young Yun. Distillm: Towards streamlined distillation for large language models. *arXiv preprint arXiv:2402.03898*, 2024.
- [20] Chen Liang, Simiao Zuo, Qingru Zhang, Pengcheng He, Weizhu Chen, and Tuo Zhao. Less is more: Task-aware layer-wise distillation for language model compression. In *International Conference on Machine Learning*, pages 20852–20867. PMLR, 2023.
- [21] Alexander Lin, Jeremy Wohlwend, Howard Chen, and Tao Lei. Autoregressive knowledge distillation through imitation learning. In *Proceedings of the 2020 Conference on Empirical Methods in Natural Language Processing (EMNLP)*, pages 6121–6133, 2020.
- [22] Chin-Yew Lin. Rouge: A package for automatic evaluation of summaries. In *Text summarization branches out*, pages 74–81, 2004.
- [23] Richard Yuanzhe Pang and He He. Text generation by learning from demonstrations. In *9th International Conference on Learning Representations, ICLR 2021*, 2021.
- [24] Kishore Papineni, Salim Roukos, Todd Ward, and Wei-Jing Zhu. Bleu: a method for automatic evaluation of machine translation. In *Proceedings of the 40th annual meeting of the Association for Computational Linguistics*, pages 311–318, 2002.
- [25] Alec Radford, Jeffrey Wu, Rewon Child, David Luan, Dario Amodei, Ilya Sutskever, et al. Language models are unsupervised multitask learners. *OpenAI blog*, 1(8):9, 2019.
- [26] Colin Raffel, Noam Shazeer, Adam Roberts, Katherine Lee, Sharan Narang, Michael Matena, Yanqi Zhou, Wei Li, and Peter J Liu. Exploring the limits of transfer learning with a unified text-to-text transformer. *Journal of machine learning research*, 21(140):1–67, 2020.
- [27] Victor Sanh, Lysandre Debut, Julien Chaumond, and Thomas Wolf. Distilbert, a distilled version of bert: smaller, faster, cheaper and lighter. *arXiv preprint arXiv:1910.01108*, 2019.
- [28] Bharath K Sriperumbudur, Kenji Fukumizu, Arthur Gretton, Bernhard Schölkopf, and Gert RG Lanckriet. On integral probability metrics, ϕ -divergences and binary classification. *arXiv preprint arXiv:0901.2698*, 2009.
- [29] Gokul Swamy, Sanjiban Choudhury, J Bagnell, and Steven Z Wu. Sequence model imitation learning with unobserved contexts. *Advances in Neural Information Processing Systems*, 35:17665–17676, 2022.
- [30] Gokul Swamy, Sanjiban Choudhury, J Andrew Bagnell, and Steven Wu. Of moments and matching: A game-theoretic framework for closing the imitation gap. In *International Conference on Machine Learning*, pages 10022–10032. PMLR, 2021.
- [31] Rohan Taori, Ishaan Gulrajani, Tianyi Zhang, Yann Dubois, Xuechen Li, Carlos Guestrin, Percy Liang, and Tatsunori B Hashimoto. Stanford alpaca: An instruction-following llama model, 2023.
- [32] Hugo Touvron, Thibaut Lavril, Gautier Izacard, Xavier Martinet, Marie-Anne Lachaux, Timothée Lacroix, Baptiste Rozière, Naman Goyal, Eric Hambro, Faisal Azhar, et al. Llama: Open and efficient foundation language models. *arXiv preprint arXiv:2302.13971*, 2023.
- [33] Yizhong Wang, Yeganeh Kordi, Swaroop Mishra, Alisa Liu, Noah A Smith, Daniel Khoshabi, and Hannaneh Hajishirzi. Self-instruct: Aligning language models with self-generated instructions. *arXiv preprint arXiv:2212.10560*, 2022.
- [34] Yizhong Wang, Swaroop Mishra, Pegah Alipoormolabashi, Yeganeh Kordi, Amirreza Mirzaei, Anjana Arunkumar, Arjun Ashok, Arut Selvan Dhanasekaran, Atharva Naik, David Stap, et al. Super-naturalinstructions: Generalization via declarative instructions on 1600+ nlp tasks. *arXiv preprint arXiv:2204.07705*, 2022.

- [35] Yuqiao Wen, Zichao Li, Wenyu Du, and Lili Mou. f-divergence minimization for sequence-level knowledge distillation. In *Proceedings of the 61st Annual Meeting of the Association for Computational Linguistics (Volume 1: Long Papers)*, pages 10817–10834, 2023.
- [36] Qingyang Wu, Lei Li, and Zhou Yu. Textgail: Generative adversarial imitation learning for text generation. In *Proceedings of the AAAI Conference on Artificial Intelligence*, volume 35, pages 14067–14075, 2021.
- [37] Taiqiang Wu, Chaofan Tao, Jiahao Wang, Zhe Zhao, and Ngai Wong. Rethinking kullback-leibler divergence in knowledge distillation for large language models. *arXiv preprint arXiv:2404.02657*, 2024.
- [38] Xiaohan Xu, Ming Li, Chongyang Tao, Tao Shen, Reynold Cheng, Jinyang Li, Can Xu, Dacheng Tao, and Tianyi Zhou. A survey on knowledge distillation of large language models. *arXiv preprint arXiv:2402.13116*, 2024.
- [39] Linting Xue, Noah Constant, Adam Roberts, Mihir Kale, Rami Al-Rfou, Aditya Siddhant, Aditya Barua, and Colin Raffel. mt5: A massively multilingual pre-trained text-to-text transformer. *arXiv preprint arXiv:2010.11934*, 2020.
- [40] Lantao Yu, Weinan Zhang, Jun Wang, and Yong Yu. Seqgan: Sequence generative adversarial nets with policy gradient. In *Proceedings of the AAAI conference on artificial intelligence*, volume 31, 2017.

A Proofs

A.1 Proof of Proposition 1

Proof. Similar to the proof of Performance Difference Lemma (PDL), we have

$$\begin{aligned}
& J(\pi_*) - J(\pi_\theta) \\
&= \mathbb{E}_{\substack{\mathbf{x} \sim p_{\mathbf{x}} \\ \tau \sim \pi_* | \mathbf{y}_0 = \mathbf{x}}} \left[\sum_{t=1}^T r(\mathbf{y}_{<t}, y_t) \right] - \mathbb{E}_{\mathbf{x} \sim p_{\mathbf{x}}} [V^{\pi_\theta}(\mathbf{x})] \\
&= \mathbb{E}_{\substack{\mathbf{x} \sim p_{\mathbf{x}} \\ \tau \sim \pi_* | \mathbf{y}_0 = \mathbf{x}}} \left[\sum_{t=1}^T (r(\mathbf{y}_{<t}, y_t) + V^{\pi_\theta}(\mathbf{y}_{<t}) - V^{\pi_\theta}(\mathbf{y}_{<t})) \right] - \mathbb{E}_{\mathbf{x} \sim p_{\mathbf{x}}} [V^{\pi_\theta}(\mathbf{x})] \\
&= \mathbb{E}_{\substack{\mathbf{x} \sim p_{\mathbf{x}} \\ \tau \sim \pi_* | \mathbf{y}_0 = \mathbf{x}}} \left[\sum_{t=1}^T (r(\mathbf{y}_{<t}, y_t) + V^{\pi_\theta}(\mathbf{y}_{<t+1}) - V^{\pi_\theta}(\mathbf{y}_{<t})) \right] \\
&\stackrel{(i)}{=} \mathbb{E}_{\substack{\mathbf{x} \sim p_{\mathbf{x}} \\ \tau \sim \pi_* | \mathbf{y}_0 = \mathbf{x}}} \left[\sum_{t=1}^T (Q^{\pi_\theta}(\mathbf{y}_{<t}, y_t) - V^{\pi_\theta}(\mathbf{y}_{<t})) \right] \\
&= \mathbb{E}_{\substack{\mathbf{x} \sim p_{\mathbf{x}} \\ \tau \sim \pi_* | \mathbf{y}_0 = \mathbf{x}}} \left[\sum_{t=1}^T \left(Q^{\pi_\theta}(\mathbf{y}_{<t}, y_t) - \mathbb{E}_{y \sim \pi_\theta(\cdot | \mathbf{y}_{<t})} [Q^{\pi_\theta}(\mathbf{y}_{<t}, y)] \right) \right] \\
&\leq \sup_{f \in \mathcal{F}_Q} \mathbb{E}_{\substack{\mathbf{x} \sim p_{\mathbf{x}} \\ \tau \sim \pi_* | \mathbf{y}_0 = \mathbf{x}}} \left[\sum_{t=1}^T \left(f(\mathbf{y}_{<t}, y_t) - \mathbb{E}_{y \sim \pi_\theta(\cdot | \mathbf{y}_{<t})} [f(\mathbf{y}_{<t}, y)] \right) \right],
\end{aligned}$$

where (i) follows from Bellman equation. \square

A.2 Proof of Proposition 2

Proof. Similar to the proof of Proposition 1, we have

$$\begin{aligned}
& J(\pi_*) - J(\pi_\theta) \\
&= - \mathbb{E}_{\substack{\mathbf{x} \sim p_{\mathbf{x}} \\ \tau \sim \pi_\theta | \mathbf{y}_0 = \mathbf{x}}} \left[\sum_{t=1}^T r(\mathbf{y}_{<t}, y_t) \right] + \mathbb{E}_{\mathbf{x} \sim p_{\mathbf{x}}} [V^{\pi_*}(\mathbf{x})] \\
&= \mathbb{E}_{\substack{\mathbf{x} \sim p_{\mathbf{x}} \\ \tau \sim \pi_\theta | \mathbf{y}_0 = \mathbf{x}}} \left[\sum_{t=1}^T (V^{\pi_*}(\mathbf{y}_{<t}) - (r(\mathbf{y}_{<t}, y_t) + V^{\pi_*}(\mathbf{y}_{<t}))) \right] + \mathbb{E}_{\mathbf{x} \sim p_{\mathbf{x}}} [V^{\pi_*}(\mathbf{x})] \\
&= \mathbb{E}_{\substack{\mathbf{x} \sim p_{\mathbf{x}} \\ \tau \sim \pi_\theta | \mathbf{y}_0 = \mathbf{x}}} \left[\sum_{t=1}^T (V^{\pi_*}(\mathbf{y}_{<t}) - (r(\mathbf{y}_{<t}, y_t) + V^{\pi_*}(\mathbf{y}_{<t+1}))) \right] \\
&= \mathbb{E}_{\substack{\mathbf{x} \sim p_{\mathbf{x}} \\ \tau \sim \pi_\theta | \mathbf{y}_0 = \mathbf{x}}} \left[\sum_{t=1}^T (V^{\pi_*}(\mathbf{y}_{<t}) - Q^{\pi_*}(\mathbf{y}_{<t}, y_t)) \right] \\
&= \mathbb{E}_{\substack{\mathbf{x} \sim p_{\mathbf{x}} \\ \tau \sim \pi_\theta | \mathbf{y}_0 = \mathbf{x}}} \left[\sum_{t=1}^T \left(\mathbb{E}_{y \sim \pi_*(\cdot | \mathbf{y}_{<t})} [Q^{\pi_*}(\mathbf{y}_{<t}, y)] - Q^{\pi_*}(\mathbf{y}_{<t+1}, y_t) \right) \right] \\
&\leq \sup_{f \in \mathcal{F}_{Q^*}} \mathbb{E}_{\substack{\mathbf{x} \sim p_{\mathbf{x}} \\ \tau \sim \pi_\theta | \mathbf{y}_0 = \mathbf{x}}} \left[\sum_{t=1}^T \left(\mathbb{E}_{y \sim \pi_*(\cdot | \mathbf{y}_{<t})} [f(\mathbf{y}_{<t}, y)] - f(\mathbf{y}_{<t+1}, y_t) \right) \right]
\end{aligned}$$

\square

A.3 Existing Step-Wise Distribution Distance for KD

Definition 4 (Step-wise distribution distances for distillation). Following Wen et al. [35], we define four groups of well-studied probability distribution distances as follows,

- **Total variation (TV) distance.** [35] *The off-policy and on-policy step-wise TV distance can be defined as follows,*

$$d_{\text{TV}}^{\text{off}}(\pi_\theta, \pi_*) := \mathbb{E}_{\substack{\mathfrak{x} \sim p_{\mathfrak{x}} \\ \tau \sim \pi_* | \mathbf{y}_0 = \mathfrak{x}}} \left[\sum_{t=1}^T \sum_{y \in \mathcal{V}} |\pi_*(y | \mathbf{y}_{<t}) - \pi_\theta(y | \mathbf{y}_{<t})| \right]; \quad (13)$$

$$d_{\text{TV}}^{\text{on}}(\pi_\theta, \pi_*) := \mathbb{E}_{\substack{\mathfrak{x} \sim p_{\mathfrak{x}} \\ \tau \sim \pi_\theta | \mathbf{y}_0 = \mathfrak{x}}} \left[\sum_{t=1}^T \sum_{y \in \mathcal{V}} |\pi_*(y | \mathbf{y}_{<t}) - \pi_\theta(y | \mathbf{y}_{<t})| \right] \quad (14)$$

- **Kullback–Leibler (KL) divergence** [35] *The off-policy and on-policy step-wise KL divergence between the teacher policy π_* and the student policy π_θ can be defined as follows,*

$$d_{\text{KL}}^{\text{off}}(\pi_*, \pi_\theta) := \mathbb{E}_{\substack{\mathfrak{x} \sim p_{\mathfrak{x}} \\ \tau \sim \pi_* | \mathbf{y}_0 = \mathfrak{x}}} \left[\sum_{t=1}^T \sum_{y \in \mathcal{V}} \pi_*(y | \mathbf{y}_{<t}) \log \frac{\pi_*(y | \mathbf{y}_{<t})}{\pi_\theta(y | \mathbf{y}_{<t})} \right]; \quad (15)$$

$$d_{\text{KL}}^{\text{on}}(\pi_*, \pi_\theta) := \mathbb{E}_{\substack{\mathfrak{x} \sim p_{\mathfrak{x}} \\ \tau \sim \pi_\theta | \mathbf{y}_0 = \mathfrak{x}}} \left[\sum_{t=1}^T \sum_{y \in \mathcal{V}} \pi_*(y | \mathbf{y}_{<t}) \log \frac{\pi_*(y | \mathbf{y}_{<t})}{\pi_\theta(y | \mathbf{y}_{<t})} \right] \quad (16)$$

- **Reverse Kullback–Leibler (RKL) divergence** [35] *The off-policy and on-policy step-wise RKL divergence between the teacher policy π_* and the student policy π_θ can be defined as follows,*

$$d_{\text{RKL}}^{\text{off}}(\pi_\theta, \pi_*) := \mathbb{E}_{\substack{\mathfrak{x} \sim p_{\mathfrak{x}} \\ \tau \sim \pi_* | \mathbf{y}_0 = \mathfrak{x}}} \left[\sum_{t=1}^T \sum_{y \in \mathcal{V}} \pi_\theta(y | \mathbf{y}_{<t}) \log \frac{\pi_\theta(y | \mathbf{y}_{<t})}{\pi_*(y | \mathbf{y}_{<t})} \right]; \quad (17)$$

$$d_{\text{RKL}}^{\text{on}}(\pi_\theta, \pi_*) := \mathbb{E}_{\substack{\mathfrak{x} \sim p_{\mathfrak{x}} \\ \tau \sim \pi_\theta | \mathbf{y}_0 = \mathfrak{x}}} \left[\sum_{t=1}^T \sum_{y \in \mathcal{V}} \pi_\theta(y | \mathbf{y}_{<t}) \log \frac{\pi_\theta(y | \mathbf{y}_{<t})}{\pi_*(y | \mathbf{y}_{<t})} \right] \quad (18)$$

- **Jenson–Shannon (JS) divergence** [35] *The JS divergence between the teacher policy π_* and the student policy π_θ can be defined based on the KL divergence and RKL divergence as follows,*

$$d_{\text{JS}}^{\text{off}}(\pi_\theta, \pi_*) := \frac{1}{2} d_{\text{KL}}^{\text{off}}(\pi_*, \frac{\pi_\theta + \pi_*}{2}) + \frac{1}{2} d_{\text{RKL}}^{\text{off}}(\pi_\theta, \frac{\pi_\theta + \pi_*}{2}); \quad (19)$$

$$d_{\text{JS}}^{\text{on}}(\pi_\theta, \pi_*) := \frac{1}{2} d_{\text{KL}}^{\text{on}}(\pi_*, \frac{\pi_\theta + \pi_*}{2}) + \frac{1}{2} d_{\text{RKL}}^{\text{on}}(\pi_\theta, \frac{\pi_\theta + \pi_*}{2}) \quad (20)$$

A.4 Proof of Corollary 1

Proof. We first derive an upper bound for the on-policy moment-matching bound of Eq. (3). Set $\mathcal{F}_{Q_*} = \{f : \|f\|_\infty \leq 1\}$, Eq. (3) can be bounded as follows,

$$\begin{aligned} & \sup_{f: \|f\|_\infty \leq 1} \mathbb{E}_{\substack{\mathfrak{x} \sim p_{\mathfrak{x}} \\ \tau \sim \pi_\theta | \mathbf{y}_0 = \mathfrak{x}}} [\mathcal{U}^{\text{on}}(\tau, f)] \\ &= \sup_{f: \|f\|_\infty \leq 1} \mathbb{E}_{\substack{\mathfrak{x} \sim p_{\mathfrak{x}} \\ \tau \sim \pi_\theta | \mathbf{y}_0 = \mathfrak{x}}} \left[\sum_{t=1}^T \left(\mathbb{E}_{y \sim \pi_*(\cdot | \mathbf{y}_{<t})} [f(\mathbf{y}_{<t}, y)] - \mathbb{E}_{y' \sim \pi_\theta(\cdot | \mathbf{y}_{<t})} [f(\mathbf{y}_{<t}, y')] \right) \right] \\ &\stackrel{(i)}{\leq} \mathbb{E}_{\substack{\mathfrak{x} \sim p_{\mathfrak{x}} \\ \tau \sim \pi_\theta | \mathbf{y}_0 = \mathfrak{x}}} \left[\sum_{t=1}^T \sup_{f: \|f\|_\infty \leq 1} \left(\mathbb{E}_{y \sim \pi_*(\cdot | \mathbf{y}_{<t})} [f(\mathbf{y}_{<t}, y)] - \mathbb{E}_{y' \sim \pi_\theta(\cdot | \mathbf{y}_{<t})} [f(\mathbf{y}_{<t}, y')] \right) \right] \\ &\stackrel{(ii)}{=} \mathbb{E}_{\substack{\mathfrak{x} \sim p_{\mathfrak{x}} \\ \tau \sim \pi_\theta | \mathbf{y}_0 = \mathfrak{x}}} \left[\sum_{t=1}^T \sum_{y \in \mathcal{V}} |\pi_*(y | \mathbf{y}_{<t}) - \pi_\theta(y | \mathbf{y}_{<t})| \right] \stackrel{\text{Def. 4}}{=} d_{\text{TV}}^{\text{on}}(\pi_\theta, \pi_*), \end{aligned}$$

where (i) follows from Jensen's inequality and (ii) follows from [28].

Similarly, we can bound the off-policy version of Eq. (2) as follows,

$$\sup_{f: \|f\|_\infty \leq 1} \mathbb{E}_{\substack{\mathbf{x} \sim p_{\mathbf{x}} \\ \tau \sim \pi_* | \mathbf{y}_0 = \mathbf{x}}} [\mathcal{U}^{\text{off}}(\tau, f, \theta)] \leq \mathbb{E}_{\substack{\mathbf{x} \sim p_{\mathbf{x}} \\ \tau \sim \pi_* | \mathbf{y}_0 = \mathbf{x}}} \left[\sum_{t=1}^T \sum_{y \in \mathcal{V}} |\pi_*(y | \mathbf{y}_{<t}) - \pi_\theta(y | \mathbf{y}_{<t})| \right]$$

$$\stackrel{\text{Def. 4}}{=} d_{\text{TV}}^{\text{off}}(\pi_\theta, \pi_*)$$

□

A.5 Derivation of Policy Gradient

Proof. Based on the definition of training objective in Eq. (9), we have

$$\begin{aligned} \nabla_\theta \mathcal{L}(\theta, \phi_1, \phi_2) &= \nabla_\theta \mathbb{E}_{\mathbf{x} \sim p_{\mathbf{x}}} \left[\mathbb{E}_{\tau \sim \pi_* | \mathbf{y}_0 = \mathbf{x}} [\mathcal{U}^{\text{off}}(\tau, f_{\phi_1}; \theta)] + \mathbb{E}_{\tau' \sim \pi_\theta | \mathbf{y}_0 = \mathbf{x}} [\mathcal{U}^{\text{on}}(\tau', f_{\phi_2})] \right] \\ &= \mathbb{E}_{\mathbf{x} \sim p_{\mathbf{x}}} \left[\mathbb{E}_{\tau \sim \pi_* | \mathbf{y}_0 = \mathbf{x}} [\nabla_\theta \mathcal{U}^{\text{off}}(\tau, f_{\phi_1}; \theta)] + \nabla_\theta \mathbb{E}_{\tau' \sim \pi_\theta | \mathbf{y}_0 = \mathbf{x}} [\mathcal{U}^{\text{on}}(\tau', f_{\phi_2})] \right] \end{aligned} \quad (21)$$

Based on the definition of $\mathcal{U}^{\text{off}}(\tau, f_{\phi_1}, \theta)$ in Eq. (2), we can compute the gradient $\nabla_\theta \mathcal{U}^{\text{off}}(\tau, f_{\phi_1}, \theta)$ for any $\tau \in \mathcal{Y}$ and $\phi_1 \in \Phi$ as follows,

$$\begin{aligned} \nabla_\theta \mathcal{U}^{\text{off}}(\tau, f_{\phi_1}, \theta) &= - \sum_{t=1}^T \nabla_\theta \mathbb{E}_{y \sim \pi_\theta(\cdot | \mathbf{y}_{<t})} [f_{\phi_1}(\mathbf{y}_{<t}, y)] \\ &= - \sum_{t=1}^T \sum_{y \in \mathcal{V}} \pi_\theta(y | \mathbf{y}_{<t}) \nabla_\theta \log \pi_\theta(y | \mathbf{y}_{<t}) f_{\phi_1}(\mathbf{y}_{<t}, y) \\ &= - \sum_{t=1}^T \mathbb{E}_{y \sim \pi_\theta(\cdot | \mathbf{y}_{<t})} \nabla_\theta \log \pi_\theta(y | \mathbf{y}_{<t}) f_{\phi_1}(\mathbf{y}_{<t}, y) \end{aligned} \quad (22)$$

then, based on the definition of $\mathcal{U}^{\text{on}}(\tau', f_{\phi_2})$ in Eq. (3), we have

$$\begin{aligned} \nabla_\theta \mathbb{E}_{\tau' \sim \pi_\theta | \mathbf{y}_0 = \mathbf{x}} [\mathcal{U}^{\text{on}}(\tau', f_{\phi_2})] &= \int \nabla_\theta [p_\theta(\tau' | \mathbf{y}_0 = \mathbf{x}) \mathcal{U}^{\text{on}}(\tau', f_{\phi_2})] d\tau' \\ &= \int \nabla_\theta p_\theta(\tau' | \mathbf{y}_0 = \mathbf{x}) \mathcal{U}^{\text{on}}(\tau', f_{\phi_2}) d\tau' \\ &= \int p_\theta(\tau' | \mathbf{y}_0 = \mathbf{x}) \nabla_\theta \log p_\theta(\tau' | \mathbf{y}_0 = \mathbf{x}) \mathcal{U}^{\text{on}}(\tau', f_{\phi_2}) d\tau' \\ &= \mathbb{E}_{\tau' \sim \pi_\theta | \mathbf{y}_0 = \mathbf{x}} [\nabla_\theta \log p_\theta(\tau' | \mathbf{y}_0 = \mathbf{x}) \mathcal{U}^{\text{on}}(\tau', f_{\phi_2})] \\ &\stackrel{(i)}{=} \mathbb{E}_{\tau' \sim \pi_\theta | \mathbf{y}_0 = \mathbf{x}} \left[\sum_{t=1}^T \nabla_\theta \log \pi_\theta(y'_t | \mathbf{y}'_{<t}) \mathcal{U}^{\text{on}}(\tau', f_{\phi_2}) \right], \end{aligned} \quad (23)$$

where (i) uses the fact that the state-transition is deterministic, and thus $\nabla_\theta \log p_\theta(\tau' | \mathbf{y}'_0 = \mathbf{x}) = \sum_{t=1}^T \nabla_\theta \log \pi_\theta(y'_t | \mathbf{y}'_{<t})$ for any $\tau' = \{y'_t | y'_t\}_{t=1, \dots, T}$.

Combining Eq. (21) with Eq. (22) and Eq. (23), we have

$$\begin{aligned} \nabla_\theta \mathcal{L}(\theta, \phi_1, \phi_2) &= \mathbb{E}_{\mathbf{x} \sim p_{\mathbf{x}}} \left[- \mathbb{E}_{\tau \sim \pi_* | \mathbf{y}_0 = \mathbf{x}} \left[\sum_{t=1}^T \mathbb{E}_{y \sim \pi_\theta(\cdot | \mathbf{y}_{<t})} \nabla_\theta \log \pi_\theta(y | \mathbf{y}_{<t}) f_{\phi_1}(\mathbf{y}_{<t}, y) \right] \right. \\ &\quad \left. + \mathbb{E}_{\tau' \sim \pi_\theta | \mathbf{y}'_0 = \mathbf{x}} \left[\sum_{t=1}^T \nabla_\theta \log \pi_\theta(y'_t | \mathbf{y}'_{<t}) \mathcal{U}^{\text{on}}(\tau', f_{\phi_2}) \right] \right] \end{aligned}$$

□

B Experimental Setup

We use NVIDIA A40 GPUs with 40GB RAM to conduct all the experiments.

B.1 Instruction-Following Experiments

Base models. We conduct experiments on both GPT-2 [25] and OpenLLaMA [9]. For the GPT-2 experiments, we use GPT-2 XL² with 1.5B parameters to construct the teacher policy and GPT-2³ with 117M parameters to construct the student policy. For the Q -value function, we use a GPT-2 model for feature extraction and add a linear layer with the size of 768 x 1 to output the logits of step y_t as $f(\mathbf{y}_{<t}, y_t)$. For the OpenLLaMA experiments, we use OpenLLaMA-7B⁴ with 6.7B parameters to construct the teacher policy and OpenLLaMA-3B⁵ with 2.7B parameters to construct the student model. We construct the Q -value function with the OpenLLaMA-3B model and a linear layer with the size of 3,200 x 1.

Training details. We fine-tune the OpenLLaMA-7B teacher model and the OpenLLaMA-3B student models on the corresponding supervised dataset with 10,000 steps. The GPT-2 teacher and student models use the fine-tuned checkpoints by Gu et al. [13]. For the implementation of compared baselines, we use the code by Ko et al. [19] and re-run the results. The optimization protocol for KD training largely follows the previous work [13; 19]. In particular, we search for the learning rates among a finite set for each experiment to obtain the best result. The batch size for each experiments is selected to make full use of the 40GB RAM of an A40 GPU. To handle the adversarial training, we choose the number of adversarial steps $K = 5$ and the adversarial control factor $\alpha = 0.1$ based on the development experiments. The hyperparameters for training are listed in Table 3.

Hyperparameter	GPT-2	OpenLLaMA
max. training steps	10,000	10,000
adv. step K	5	5
batch size (per GPU)	{8, 16, 32}	{4, 8}
dropout rate	0.1	0.1
adv. control factor (α)	0.1	0.1
learning rate (lr)	{ $5e^{-5}$, $1e^{-4}$, $5e^{-4}$ }	{ $5e^{-6}$, $1e^{-5}$, $5e^{-5}$ }
warmup steps	1,000	500
weight decay	$1e^{-2}$	$1e^{-2}$
max length	512	512
sampling top-p	1.0	1.0
sampling temperature	1.0	1.0
evaluation	Greedy Sampling	Greedy Sampling
#GPUs	2	4

Table 3: Training hyperparameters for instruction-following experiments.

B.2 Task-Specific Experiments

Base models. For the text summarization and commonsense reasoning experiments, we use T5-XL⁶ with 2.8B parameters to construct the teacher policy and construct the student policy with T5-Large⁷ (770M parameters), T5-Base⁸ (220M parameters) and T5-Small⁹ (60M parameters). For the machine translation experiments, we use mT5-XL [39] to construct the teacher policy and use mT5-Large/-Base/-Small to construct the student policy. The corresponding Q -value functions are constructed using the student model and a linear layer of size 1024x1, 768x1 and 512x1 for the large, base and small models, respectively.

²<https://huggingface.co/openai-community/gpt2-xl>

³<https://huggingface.co/openai-community/gpt2>

⁴https://huggingface.co/openlm-research/open_llama_7b

⁵https://huggingface.co/openlm-research/open_llama_7b

⁶https://huggingface.co/google/t5-v1_1-xl

⁷https://huggingface.co/google/t5-v1_1-large

⁸https://huggingface.co/google/t5-v1_1-base

⁹https://huggingface.co/google/t5-v1_1-small

Training details We initialize the corresponding teacher and student models using 10,000-step-fine-tuning checkpoints on the SAMSum dataset, 80,000-step-fine-tuning checkpoints on the IWSLT’17 (en-de) dataset and 3,000-step-fine-tuning checkpoints on the StrategyQA dataset. We largely follow Ko et al. [19] to set the hyperparameters for training. In particular, we search for the learning rate from a preset range to obtain the best result for each baseline and our method. The batch size is selected to make full use of the RAM of GPUs. We use a relatively larger maximum number of training steps for IWSLT’17 (en-de) experiments to satisfy sufficient convergences for the machine translation task. We use beam search for the evaluation on the IWSLT’17 (en-de) dataset.

Hyperparameter	SAMSum	IWSLT’17 (en-de)	StrategyQA
max. training steps	10,000	80,000	3,000
adv. step K	5	2	5
batch size (per GPU)	{16, 32, 64}	{16, 32, 64}	{16, 32, 64}
dropout rate	0.0	0.3	0.1
adv. control factor (α)	0.1	0.1	0.1
learning rate (lr)	{ $5e^{-5}$, $1e^{-4}$, $5e^{-4}$ }	{ $1e^{-4}$, $5e^{-4}$, $1e^{-3}$ }	{ $1e^{-4}$, $5e^{-4}$, $1e^{-3}$ }
warmup steps	1,000	4,000	300
weight decay	$1e^{-2}$	$1e^{-4}$	$1e^{-2}$
max. length	1024	512	1,024
sampling top-p	1.0	1.0	1.0
sampling temperature	1.0	1.0	1.0
evaluation	Greedy sampling	Beam search	Greedy sampling
#GPUs	2	4	1

Table 4: Training hyperparameters on three task-specific datasets.

C Additional Results

C.1 Results Based on GPT-2

In addition to the experimental results based on OpenLLaMA for instruction-following tasks, we also conduct experiments based on GPT-2. Results are illustrated in Table 5. Compared with current state-of-the-art KD approaches, our method achieves the best results on five datasets with both GPT-4 feedback and ROUGE-L evaluations.

Method	DollyEval		SelfInst		VicunaEval		S-NI	UnNI
	GPT4	R-L	GPT4	R-L	GPT4	R-L	R-L	R-L
<i>GPT-2 XL (teacher)</i>	<i>45.5\pm0.7</i>	<i>28.2\pm0.8</i>	<i>34.7\pm1.6</i>	<i>14.3\pm0.2</i>	<i>32.7\pm1.6</i>	<i>16.2\pm0.3</i>	<i>27.6\pm0.3</i>	<i>32.2\pm0.3</i>
SFT (student)	29.8 \pm 1.2	23.4 \pm 0.2	20.2 \pm 0.7	10.3 \pm 0.5	17.8 \pm 0.9	14.6 \pm 0.4	16.1 \pm 0.3	18.2 \pm 0.6
KD [15]	29.5 \pm 0.8	23.8 \pm 0.3	18.0 \pm 1.0	12.3 \pm 0.2	17.2 \pm 0.7	15.2 \pm 0.4	20.8 \pm 0.5	22.5 \pm 0.3
SeqKD [18]	29.8 \pm 0.5	24.2 \pm 0.2	18.2 \pm 0.8	11.6 \pm 0.4	18.2 \pm 0.7	15.5 \pm 0.3	15.5 \pm 0.6	20.1 \pm 0.1
ImitKD [21]	26.4 \pm 0.6	22.7 \pm 0.5	18.2 \pm 0.5	11.5 \pm 0.4	18.6 \pm 0.4	14.5 \pm 0.3	18.2 \pm 0.3	21.8 \pm 0.4
MiniLLM [13]	30.2 \pm 1.2	24.3 \pm 0.3	20.5 \pm 0.3	13.2 \pm 0.3	20.5 \pm 0.7	18.5 \pm 0.3	22.7 \pm 0.3	23.5 \pm 0.2
GKD [2]	29.2 \pm 0.6	23.6 \pm 0.2	20.7 \pm 0.5	12.7 \pm 0.2	20.2 \pm 0.6	17.7 \pm 0.2	25.1 \pm 0.3	25.9 \pm 0.1
DistiLLM [19]	31.2 \pm 0.4	25.2 \pm 0.4	21.7 \pm 0.5	12.5 \pm 0.3	22.5 \pm 1.2	19.2 \pm 0.5	27.7 \pm 0.2	27.6 \pm 0.4
ours	31.7\pm0.5	26.1\pm0.3	22.7\pm0.5	14.2\pm0.3	23.6\pm0.8	20.5\pm0.2	28.6\pm0.2	29.9\pm0.5

Table 5: Comparison with state-of-the-art KD methods on the instruction-following dataset using fine-tuned GPT-2 XL (1.5B) as the teacher and fine-tuned GPT-2 (0.1B) as the student. We format **the best**, the second best and worse than SFT results.

C.2 Comparisons on Step-Wise Distribution Distance

Figure 4 and Figure 5 illustrate performance comparison with well-studied step-wise distribution distance, including KL, RKL, JS divergences and TV distances. Results show that the optimization of proposed moment-matching objectives outperforms other step-wise distribution distances via either on-policy distillation and off-policy distillation. Besides, jointly using on-policy and off-policy

moment-matching further improves the performances and achieves the best results on five instruction-following datasets with KD from the OpenLLaMA-7B to OpenLLaMA-3B model, and achieves the best results on three task-specific datasets with KD from the (m)T5-XL to (m)T5-Base model.

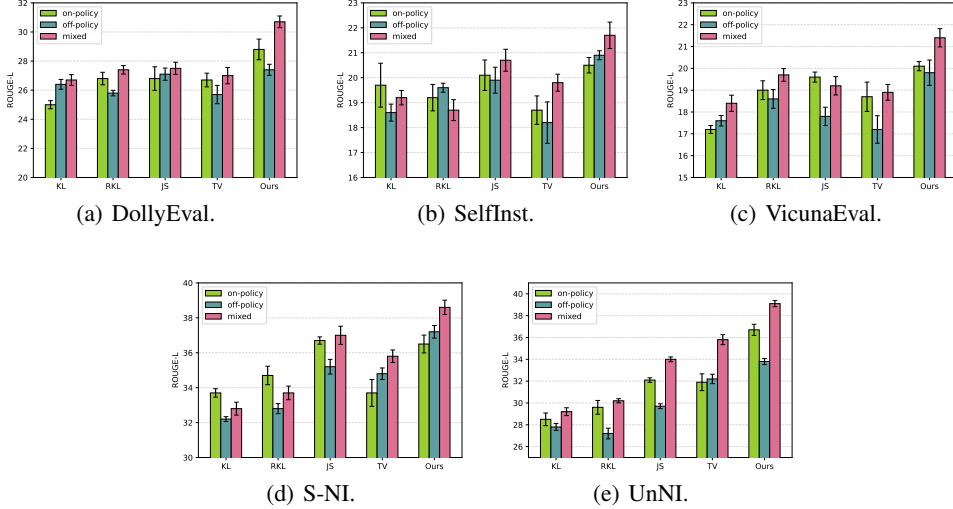


Figure 4: Performance of difference step-wise distribution distances on five instruction-following datasets based on OpenLLaMA-3B \rightarrow OpenLLaMA-7B.

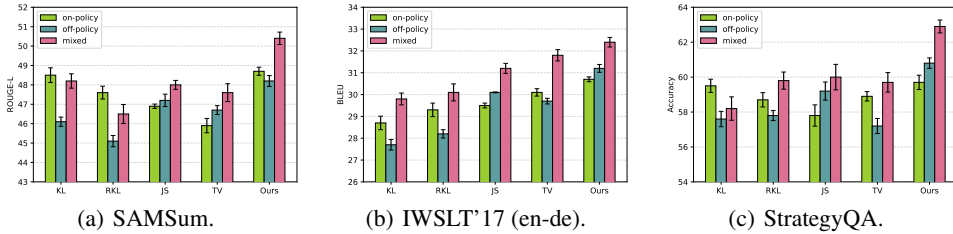


Figure 5: Performance of difference step-wise distribution distances on three task-specific datasets based on (m)T5-XL \rightarrow (m)T5-Base.

C.3 Adversarial Training Procedure

Figure 6 illustrates the training loss and on/off-policy moment-matching distances against the training steps on the instruction-following dataset and three task-specific datasets. We can observe that the training losses on four datasets have a similar trend, increasing at the beginning and then converging to a relatively lower level. The trend of loss function aligns with the characteristics of adversarial training with gradient descent ascent. In contrast, both the on-policy moment-matching distance d_{MM}^{on} and the off-policy moment-matching distance d_{MM}^{off} reduce as the number of training steps increases, which shows the effectiveness of our adversarial training approach for moment-matching.

C.4 Moment-Matching via Distribution Matching

We investigate how the distribution-matching methods via KL, RKL, JS divergences or TV distance can optimize the moment-matching distance in Figure 7 and Figure 8. Results show that the proposed adversarial training algorithm are more effective in minimizing the moment-matching distance than the distribution-matching methods.

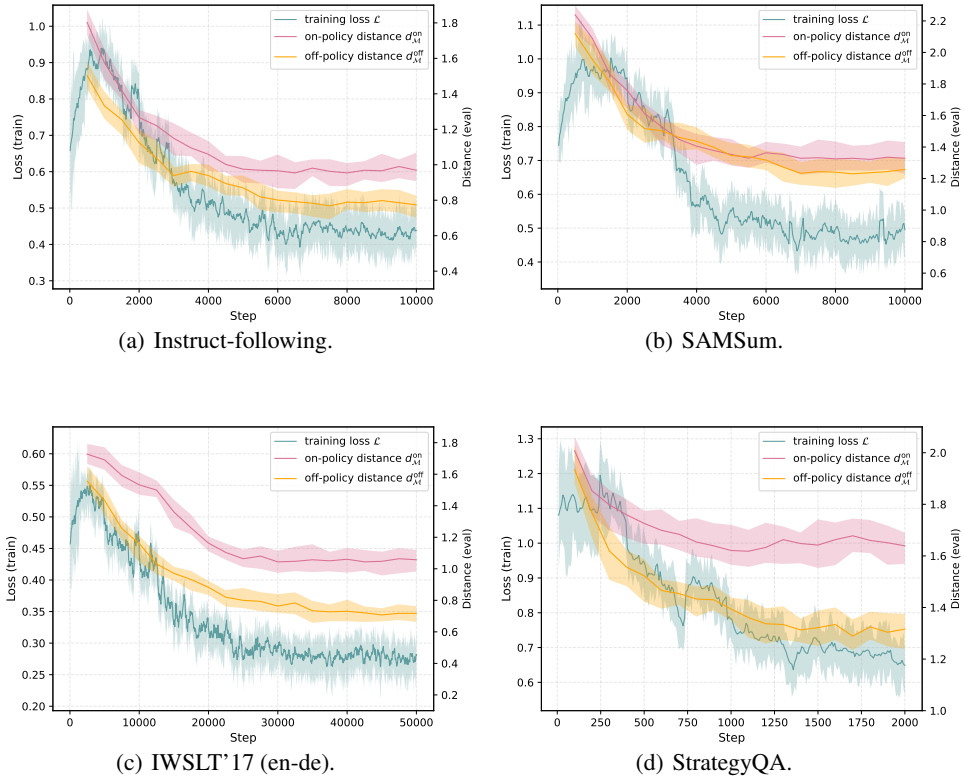


Figure 6: Training loss and d_{MM}^{on} , d_{MM}^{off} against training step on four datasets.

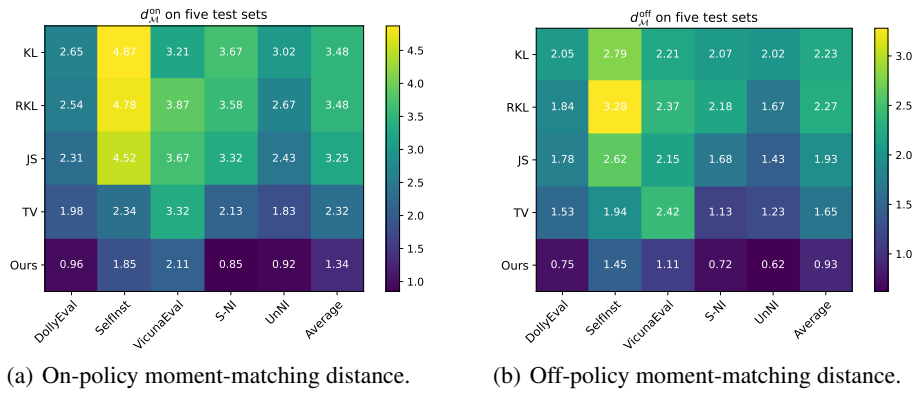


Figure 7: Moment-matching via distribution-matching on the instruction-following dataset.

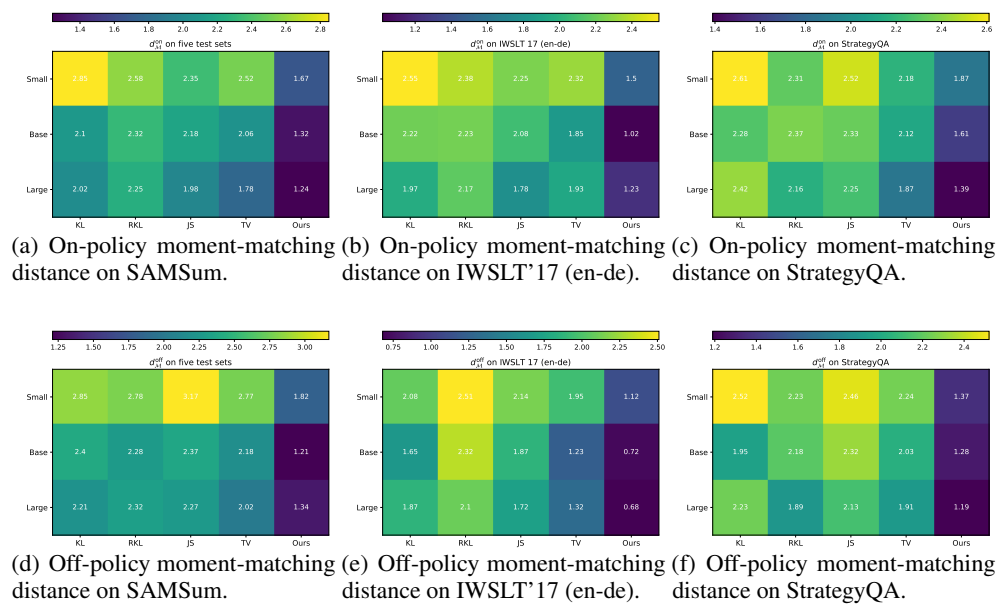


Figure 8: Moment-matching via distribution-matching on three task-specific datasets.